

Synthesis of PbS nanocrystallites using a novel single molecule precursors approach: X-ray single-crystal structure of Pb(S₂CNEtPrⁱ)₂

Tito Trindade,^{a,†} Paul O'Brien,^{a,‡} Xiao-mei Zhang^b and Majid Motevalli^c

^aDepartment of Chemistry, Imperial College of Science, Technology and Medicine, London, UK SW7 2AY

^bThe Interdisciplinary Research Centre for Semiconductor Materials, The Blakett Laboratory, Imperial College of Science, Technology and Medicine, London, UK SW7 2BZ

^cDepartment of Chemistry, Queen Mary & Westfield College, London, UK E1 4NS

The synthesis and characterisation of some lead(II) dithiocarbamate complexes Pb(S₂CNRR')₂ is reported. These compounds were used as single molecule precursors to produce nanocrystalline PbS by their thermolysis in trioctylphosphine oxide. The optical and morphological properties of the resulting PbS nanocrystallites were investigated; the influence of experimental parameters, such as precursor, growth time and temperature, on the final nanodispersed materials is also reported.

The last decade has seen intense research into the synthesis and characterisation of semiconductor nanocrystallites. Nanocrystallites have electro-optical and mechanical properties distinct from macrocrystalline materials and are promising materials for several technological applications.^{1–6}

Nanocrystalline PbS is a semiconductor that has received some attention and a number of studies related to the synthesis and optical characterisation of this material can be found in the literature.^{7–13} However, unlike II–VI semiconductors (*e.g.* CdS and CdSe) which have been prepared by a wide range of synthetic procedures^{1–6} most of the methods employed, to date, for the synthesis of PbS nanocrystallites are based on traditional precipitation techniques in aqueous media^{7–9} or by crystallisation in structures such as zeolites¹⁰ or polymers.^{11–13} We report here a novel method for the preparation of nanocrystalline PbS which uses the thermolysis of single molecule precursors in tri-*n*-octylphosphine oxide (TOPO). A similar method has been used in our laboratories to synthesise CdS or CdSe nanocrystallites.¹⁴ High-quality nanocrystallites have been prepared by using TOPO as a dispersing medium either by the single-source¹⁴ or by the two-precursors approach of Bawendi and co-workers.¹⁵ Although there is a report on the preparation of bulk PbS from lead bis(butylthiolate),¹⁶ to the best of our knowledge the synthesis of nanodispersed PbS using a single molecule precursor has not been reported before. However, this case is one in which the single-source approach is clearly advantageous because the use of poisonous compounds such as H₂S or lead alkyls is avoided.

Lead dithiocarbamate complexes have received little attention as potential precursors for the production of PbS materials.¹⁷ In this paper we describe the use of such precursors for the production of PbS nanocrystallites. The optical and structural properties of the nanoparticulates were evaluated by optical absorption measurements and high-resolution transmission electron microscopy (HRTEM). The influence of experimental parameters on the final properties of the nanocrystallites is also discussed.

Experimental

Synthesis of lead(II) dithiocarbamate complexes

Pb(NO₃)₂, ethanol (99.7–100%), dichloromethane and CS₂ were from BDH. All other chemicals were from Aldrich. TOPO

(90%, Aldrich) was purified by the method described in the literature.¹⁸ All other chemicals were used as received.

Pb(S₂CNEt₂)₂ was synthesised by the stoichiometric reaction of 0.1 mol dm⁻³ aqueous solutions of Pb(NO₃)₂ (50 ml) and Na(S₂CNEt₂) (50 ml). The pale yellow precipitate was then washed thoroughly with distilled water and dried at room temperature. All the other lead complexes were synthesised by the insertion of CS₂ into the respective secondary amine, in the presence of a suspension of freshly prepared yellow PbO in ethanol. In a typical synthesis Pb(S₂CNEtPrⁱ)₂ was prepared by adding 0.23 cm³ (4.13 mmol) of CS₂ to 50 ml of an ethanolic suspension containing 0.5 cm³ (4.13 mmol) of *N*-ethylisopropylamine and 0.5 g (2.07 mmol) of yellow PbO. The mixture was stirred overnight at room temperature; after addition of 10 ml of CH₂Cl₂ to the solution any unreacted PbO was removed by filtration. The solvent was then evaporated under reduced pressure. Crystals of Pb(S₂CNEtPrⁱ)₂ suitable for crystallography were obtained on recrystallisation of the compound in hot toluene (90 °C).

Pb(S₂CNEt₂)₂, ¹H NMR, δ 1.33 (3H, t, CH₂CH₃), 3.80 (2H, q, CH₂CH₃); ¹³C NMR, δ 12.29 (CH₂CH₃), 47.31 (CH₂CH₃), 202.17 (S₂CN); IR and Raman, ν/cm⁻¹ (major bands, Raman bands in italic and tentative assignments): 1483, 1489 [ν(C–N)]; 983, 987 [ν(C–S)]; 357, 362 [ν(Pb–S)]; yield: 93%.

Pb(S₂CNEtPrⁱ)₂, ¹H NMR, δ 1.37 (3H, t, CH₂CH₃), 3.72 (2H, q, CH₂CH₃), 1.31 [6H, d, CH(CH₃)₂], 5.47 [1H, m, CH(CH₃)₂]; ¹³C NMR, δ 14.38 (CH₂CH₃), 20.00 [CH(CH₃)₂], δ 41.42 (CH₂CH₃), 53.28 [CH(CH₃)₂], 202.23 (S₂CN); IR and Raman, ν/cm⁻¹: 1472, 1464 [ν(C–N)]; 987, 986 [ν(C–S)]; 358, 374 [ν(Pb–S)]; yield: 53%.

Pb(S₂CNMeBuⁿ)₂, ¹H NMR, δ 0.95 [3H, t, (CH₂)₃CH₃], 1.36 [2H, m, (CH₂)₂CH₂CH₃], δ 1.73 (2H, m, CH₂CH₂CH₂CH₃), 3.32 (3H, s, CH₃), 3.76 [2H, t, CH₂(CH₂)₂CH₃]; ¹³C NMR, δ 13.83 [(CH₂)₃CH₃], 20.13 [(CH₂)₂CH₂CH₃], 29.02 (CH₂CH₂CH₂CH₃), 40.78 (CH₃), δ 55.19 [CH₂(CH₂)₂CH₃], 203.15 (S₂CN); IR and Raman, ν/cm⁻¹: 1491, 1490 [ν(C–N)]; 960, 960 [ν(C–S)], 357, 358 [ν(Pb–S)]; yield: 58%.

Pb(S₂CNBuⁿ)₂, ¹H NMR, δ 0.95 [3H, t, (CH₂)₃CH₃], 1.35 [2H, m, (CH₂)₂CH₂CH₃], 1.75 (2H, m, CH₂CH₂CH₂CH₃), 3.70 [2H, t, CH₂(CH₂)₂CH₃]; ¹³C NMR, δ 13.77 [(CH₂)₃CH₃],

† Present address: Department of Chemistry, University of Aveiro, 3810 Aveiro, Portugal.

‡ E-mail: p.obrien@ic.ac.uk

Table 1 Properties of some Pb(S₂CNRR')₂ complexes

compound	R	R'	colour	mp/°C	analysis ^a (%)			m/z ^b
					C	H	N	
Pb(S ₂ CNEt) ₂	Et	Et	pale yellow	208	23.7 (23.8)	3.8 (4.0)	5.5 (5.6)	356 {PbS ₂ CNEt ₂ } ⁺
Pb(S ₂ CNEtPr ⁱ) ₂	Et	Pr ⁱ	pale yellow	127	27.1 (27.3)	4.2 (3.8)	5.3 (5.3)	370 {PbS ₂ CNEtPr ⁱ } ⁺
Pb(S ₂ CNMeBu ⁿ) ₂	Me	Bu ⁿ	white	98	27.2 (27.1)	4.5 (4.6)	5.2 (5.3)	370 {PbS ₂ CNMeBu ⁿ } ⁺
Pb(S ₂ CNBu ⁿ) ₂	Bu ⁿ	Bu ⁿ	pale yellow	76	35.1 (35.1)	5.6 (5.9)	4.5 (4.6)	412 {PbS ₂ CNBu ⁿ } ⁺
Pb(S ₂ CNBu ⁱ) ₂	Bu ⁱ	Bu ⁱ	pale yellow	98	34.0 (35.1)	5.1 (5.9)	4.5 (4.6)	412 {PbS ₂ CNBu ⁱ } ⁺
Pb[S ₂ CNMe(<i>n</i> -C ₆ H ₁₃)] ₂	Me	<i>n</i> -C ₆ H ₁₃	pale yellow	87	33.9 (32.7)	5.8 (5.5)	5.1 (4.8)	398 {PbS ₂ CNMe(<i>n</i> -C ₆ H ₁₃)} ⁺

^aCalculated values in parentheses. ^bStrongest peak in the mass spectrum.

20.23 [(CH₂)₂CH₂CH₃], 29.06 (CH₂CH₂CH₂CH₃), 52.92 [CH₂(CH₂)₂CH₃], 202.49 (S₂CN); IR and Raman, ν/cm^{-1} : 1478, 1477 [$\nu(\text{C}-\text{N})$]; 961, 961 [$\nu(\text{C}-\text{S})$]; 359, 372 [$\nu(\text{Pb}-\text{S})$]; yield: 56%.

Pb(S₂CNBuⁱ)₂. ¹H NMR, δ 0.95 [6H, d, (CH₂CH(CH₃)₂)₂], 2.46 [1H, m, CH₂CH(CH₃)₂], 3.62 [2H, d, CH₂CH(CH₃)₂]; ¹³C NMR, δ 20.37 [CH₂CH(CH₃)₂], 27.07 [CH₂CH(CH₃)₂], 60.64 [CH₂CH(CH₃)₂], 204.55 (S₂CN); IR and Raman, ν/cm^{-1} : 1475, 1479 [$\nu(\text{C}-\text{N})$]; 972, 960 [$\nu(\text{C}-\text{S})$]; 341, 369 [$\nu(\text{Pb}-\text{S})$]; yield: 46%.

Pb[S₂CNMe(*n*-C₆H₁₃)]₂. ¹H NMR, 0.89 [3H, t, (CH₂)₅CH₃], 1.30 [6H, m, (CH₂)₂(CH₂)₃CH₃], 1.74 [2H, m, CH₂CH₂(CH₂)₃CH₃], 3.32 (3H, s, CH₃), δ 3.75 [2H, t, CH₂(CH₂)₄CH₃]; ¹³C NMR, δ 14.05 [(CH₂)₅CH₃], 22.58 [(CH₂)₄CH₂CH₃], 26.51 [(CH₂)₃CH₂CH₂CH₃], 26.87 [(CH₂)₂CH₂(CH₂)₂CH₃], 31.49 [CH₂CH₂(CH₂)₃CH₃], 40.82 (CH₃), 55.45 [CH₂(CH₂)₄CH₃], 202.98 (S₂CN); IR and Raman, ν/cm^{-1} : 1491, 1488 [$\nu(\text{C}-\text{N})$]; 964, 968 [$\nu(\text{C}-\text{S})$]; 357, 360 [$\nu(\text{Pb}-\text{S})$]; yield: 76%.

Table 1 lists other properties for the above complexes. Microanalysis was carried out in the Microanalytical Laboratories at Imperial College.

Synthesis of PbS nanocrystallites

The PbS nanocrystallites were synthesised by injecting solutions of Pb(S₂CNRR')₂ [in toluene or trioctylphosphine (TOP)] into TOPO at a required temperature (e.g. 150 °C) under an atmosphere of nitrogen.

In a typical preparation, Pb(S₂CNBuⁱ)₂ (0.12 mmol, 0.075 g) was dissolved in 5 ml of toluene. This solution was carefully injected into 30 g of TOPO, while stirring at 100–150 °C (**CAUTION**: at normal pressure the boiling point of toluene is 111 °C). The reaction vessel, a three-necked tubular flask, was connected *via* a lateral neck to a flask equipped with a Liebig condenser in order to remove any toluene from the reactant solution. After heating (e.g. for 1 h) the grey mixture was allowed to cool to 70 °C and an excess of MeOH was added. The solid was then isolated by centrifugation, washed with MeOH (10 ml) and dried under vacuum. The synthesis of PbS nanocrystallites at 200 and 250 °C was carried out by injecting the precursor at 150 °C and then slowly increasing the temperature. TOP could be used instead of toluene but a loss of the solubility of the precursor was observed.

The formation of nanocrystallites with heating time was monitored by recording the optical absorption spectra of aliquots (2 ml) collected with a syringe from the reactant

solution, addition of an excess of MeOH, centrifugation and redispersion in toluene.

The synthesis of PbS nanocrystallites using other molecular precursors was carried out using similar synthetic procedures.

Instrumentation and physical measurements

Crystallography. Intensity data were collected on an Enraf-Nonius CAD-4 diffractometer operating in the ω - 2θ scan mode, with graphite-monochromated Mo-K α radiation. The unit-cell parameters were determined by least-squares refinements on positions of 25 automatically centred reflections with $10 \leq \theta \leq 14^\circ$. The structures were solved by the direct method using the SHELX program package¹⁹ and refined anisotropically on F^2 by full-matrix least-squares procedures using the SHELXL-93 package.²⁰ The crystal data and structure refinement data for Pb(S₂CNEtPrⁱ)₂ are shown in Table 2. All H atoms were placed at calculated positions by using AFIX command in SHELXL-93 (riding model). Displacement parameters of H atoms were kept fixed at the isotropic values of the parent atoms. Atomic coordinates, thermal parameters, and bond lengths and angles have been deposited at the Cambridge Crystallographic Data Centre (CCDC). See

Table 2 Crystal data and structure refinement of Pb(S₂CNEtPrⁱ)₂

empirical formula	C ₁₂ H ₂₄ N ₂ PbS ₄
formula mass	531.76
temperature/K	293(2)
wavelength/Å	0.71069
crystal system	monoclinic
space group	<i>C</i> / <i>c</i>
unit-cell dimensions	
<i>a</i> /Å	22.478(4)
<i>b</i> /Å	9.718(2)
<i>c</i> /Å	8.734(2)
β /degrees	102.62(3)
volume/Å ³	1861.8(7)
<i>Z</i>	4
<i>D_c</i> /g cm ⁻³	1.897
absorption coefficient/mm ⁻¹	9.501
<i>F</i> (100)	1024
crystal size/mm ³	0.45 × 0.25 × 0.13
θ range for data collection/degrees	1.86–24.97
index range <i>hkl</i>	–26 to 26, –5 to 11, –10 to 3
reflections collected	1818
independent reflections (<i>R</i> _{int})	1771 (0.0122)
refinement method	full-matrix least-squares on F^2
data/restraints/parameters	1770/2/189
goodness-of-fit on F^2	1.096
final <i>R</i> indices [$I > 2\sigma(I)$]	<i>R</i> ₁ = 0.0289, <i>wR</i> ₂ = 0.0717
<i>R</i> indices (all data)	<i>R</i> ₁ = 0.0446, <i>wR</i> ₂ = 0.0752
largest difference peak, hole/e Å ⁻³	0.885, –0.839

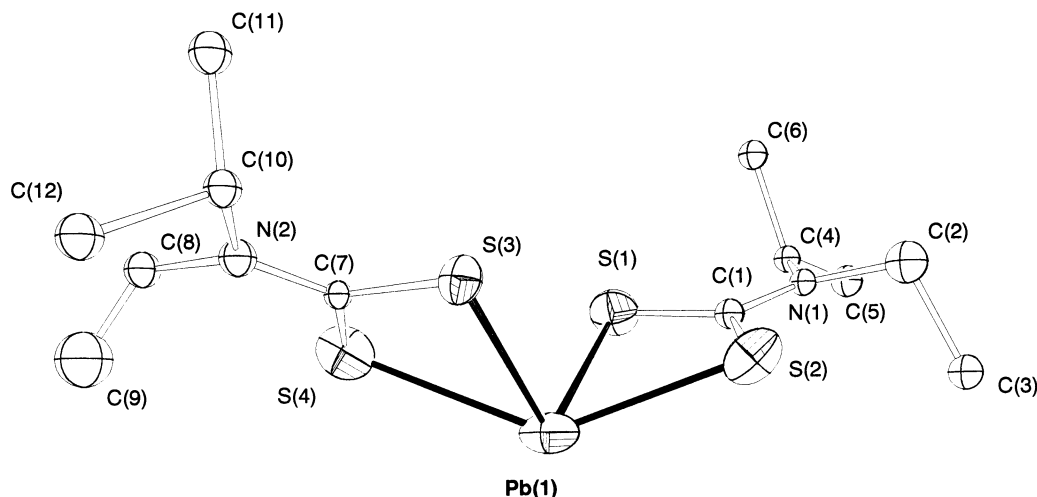


Fig. 1 X-Ray single-crystal structure of $\text{Pb}(\text{S}_2\text{CNEtPr})_2$

Information for Authors, *J. Mater. Chem.*, 1997, Issue 1. Any request to the CCDC for this material should quote the full literature citation and the reference number 1145/35.

Spectroscopic measurements. ^1H NMR and $^{13}\text{C}\{^1\text{H}\}$ NMR spectra were recorded on a JEOL ESX 270 or on a Brüker WM-250 FT using CDCl_3 - SiMe_4 as solvent. IR spectra were recorded on a Matson instrument using CsI disks. Raman spectra were measured as powders on a Perkin-Elmer 1760X FTIR instrument fitted with a 1700X NIR FT-Raman accessory (Spectron Nd: YAG laser, 1064 nm excitation). Mass spectra were recorded on a VG Autospec, using for positive FAB a Cs^+ primary ion beam (30 keV) and using a 3-nitrobenzyl alcohol matrix.

Electron microscopy and electron diffraction. HRTEM images and transmission electron diffraction patterns were obtained using a JEOL-JEM-2010 electron microscope operating at 200 kV. Samples were prepared by placing an aliquot of a toluene solution containing PbS nanocrystallites onto a carbon-coated copper grid and then allowing the solvent to evaporate at room temperature. Measurements of the dimensions of the nanoparticles were performed directly using the HRTEM images. In order to index the electron diffraction patterns, the camera constant was determined using an aluminium standard.

Results and Discussion

Single molecule precursors

There are a few papers reporting the synthesis and thermal behaviour of lead(II) dithiocarbamates.^{21–24} The X-ray single-crystal structures of $\text{Pb}(\text{S}_2\text{CNR}_2)_2$, $\text{R} = \text{Me}$,²⁵ Et ,^{26,27} and Pr^i ²⁸ have been reported. These compounds, however, are far from being fully characterised.

The crystal structure of $\text{Pb}(\text{S}_2\text{CNEtPr}^i)_2$ is shown in Fig. 1. This compound has two different alkyl substituents on the nitrogen but has a crystal structure core similar to those of $\text{Pb}(\text{S}_2\text{CNMe}_2)_2$, $\text{Pb}(\text{S}_2\text{CNEt}_2)_2$ and $\text{Pb}(\text{S}_2\text{CNEtPr}^i)_2$, which were reported previously.^{25–28} The lead atom is coordinated to four sulfur atoms, two from each ethylisopropylthiocarbamate chelating ligand. The total number of sulfur atoms surrounding each lead atom is six if short intermolecular contacts, with two different neighbouring molecules are considered (Fig. 2, Table 3). The intermolecular distances $\text{Pb}(1)\cdots\text{S}'(1)$ [3.488(2) Å] and $\text{Pb}(1)\cdots\text{S}(3)$ [3.497(2) Å] are longer than a covalent $\text{Pb}-\text{S}$ bond but shorter than the sum

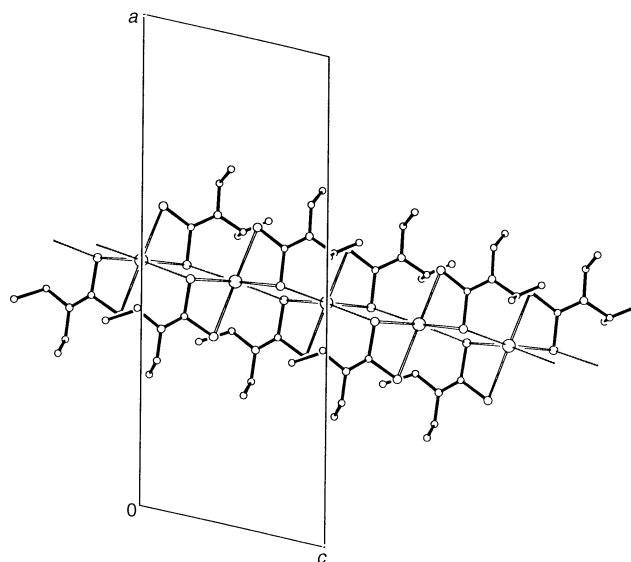


Fig. 2 Molecular packing diagram of $\text{Pb}(\text{S}_2\text{CNEtPr}^i)_2$

Table 3 Selected bond lengths (Å) and angles (degrees) for $\text{Pb}(\text{S}_2\text{CNEtPr}^i)_2$

$\text{Pb}(1)-\text{S}(3)$	2.675(2)	$\text{S}(3)-\text{Pb}(1)-\text{S}(1)$	99.11(4)
$\text{Pb}(1)-\text{S}(1)$	2.714(2)	$\text{S}(3)-\text{Pb}(1)-\text{S}(2)$	89.32(7)
$\text{Pb}(1)-\text{S}(2)$	2.862(3)	$\text{S}(1)-\text{Pb}(1)-\text{S}(2)$	64.36(6)
$\text{Pb}(1)-\text{S}(4)$	2.880(3)	$\text{S}(3)-\text{Pb}(1)-\text{S}(4)$	63.78(7)
$\text{Pb}(1)\cdots\text{S}'(1)$	3.488(2)	$\text{S}(1)-\text{Pb}(1)-\text{S}(4)$	88.24(6)
$\text{Pb}(1)\cdots\text{S}'(1)$	3.497(2)	$\text{S}(2)-\text{Pb}(1)-\text{S}(4)$	138.60(5)

of van der Waals radii (3.82 Å).²⁹ This type of environment is similar to that one observed for the lead atom in $\text{Pb}(\text{S}_2\text{CNEtPr}^i)_2$;²⁸ for $\text{Pb}(\text{S}_2\text{CNEt}_2)_2$ two of the six sulfur atoms surrounding the metal atom (and forming intermolecular contacts) belong to the same neighbouring molecule.²⁷ Fig. 2 shows that the molecular units of $\text{Pb}(\text{S}_2\text{CNEtPr}^i)_2$ are aligned along the c axis, similar to $\text{Pb}(\text{S}_2\text{CNEt}_2)_2$ ^{26,27} and $\text{Pb}(\text{S}_2\text{CNMe}_2)_2$,²⁵ and in contrast to $\text{Pb}(\text{S}_2\text{CNEtPr}^i)_2$ in which a linear-chain structure along the b axis is formed.²⁸ The four $\text{Pb}-\text{S}$ distances in the compound $\text{Pb}(\text{S}_2\text{CNEtPr}^i)_2$ (Table 3) are different and the sulfur atoms are non-coplanar. The relative bond distances and bond angles (Table 3) for $\text{Pb}(\text{S}_2\text{CNEtPr}^i)_2$ agree with the presence of an electron lone

pair (E) at an equatorial position of a distorted trigonal-bipyramid PbS_4E . Evidence for the presence of a stereochemically active electron lone pair at the lead atom has also been reported for other lead complexes.^{30,31}

The vibrational data showed the characteristic bands for the compounds. The strong bands in the region $1460\text{--}1500\text{ cm}^{-1}$ were assigned to the stretching of the C–N bond, which has polar characteristics and is intermediate between a single and double bond. In the region of the C–S stretching vibration, $960\text{--}1000\text{ cm}^{-1}$, only a strong band was found in the vibrational spectra for the dithiocarbamate complexes, which is expected if the bidentate ligands are chelated to the lead atom and do not have a free C–S bond.³² The Pb–S stretching vibration was assigned to the IR and Raman bands found in the low-frequency region $300\text{--}380\text{ cm}^{-1}$. These bands were generally weak in the IR and of medium intensity in the Raman spectra. Xanthate, dithiooxalate and dithiocarbamate complexes show the metal–sulfur stretching mode at $288\text{--}436\text{ cm}^{-1}$.^{33–35} The assignment of $\nu(\text{Pb–S})$ to the stronger bands observed in this spectral region was made on that basis,³³ although the same authors have reported³⁴ that $\nu(\text{Pb–S})$ can be low as 170 cm^{-1} in lead thiourea complexes, containing the non-charged thiourea ligand.

A decrease in the melting point of the compounds was observed as the alkyl groups become longer or/and asymmetrical. Similar behaviour has been observed for zinc and cadmium dithiocarbamate complexes,^{36,37} and may be explained by an increase of the steric hindrance of the ligand, weakening the intermolecular forces within the compounds.

Optical properties of PbS nanocrystallites

The $\text{Pb}(\text{S}_2\text{CNRR}')_2$ complexes when dispersed in hot TOPO decomposed to give a brown–grey material. After injection of the precursor into hot TOPO (*e.g.* 150°C) the solution changed in a matter of 10–30 min from pale yellow to brownish–grey and, over longer times, to black. Fig. 3 shows the optical absorption spectra of nanodispersed PbS in toluene obtained from the thermolysis of different $\text{Pb}(\text{S}_2\text{CNRR}')_2$ precursors in TOPO. The optical properties of the PbS suspensions prepared are similar from all precursors (Fig. 3), if other experimental conditions remain constant. It was found that the temperature of injection, and growth time, have much more effect on the optical absorption spectra of nanodispersed PbS than the nature of the precursors used (Fig. 4). Using the same precursor, *e.g.* $\text{Pb}(\text{S}_2\text{CNBu}^i)_2$, the absorption tail steepens for PbS synthesised at 100°C as compared to 150°C . A similar result was observed for samples prepared for shorter heating times (Fig. 5). The optical spectra for all the samples of PbS analysed, independent of the synthetic conditions used, were featureless and a smooth decrease in the optical absorption from the near

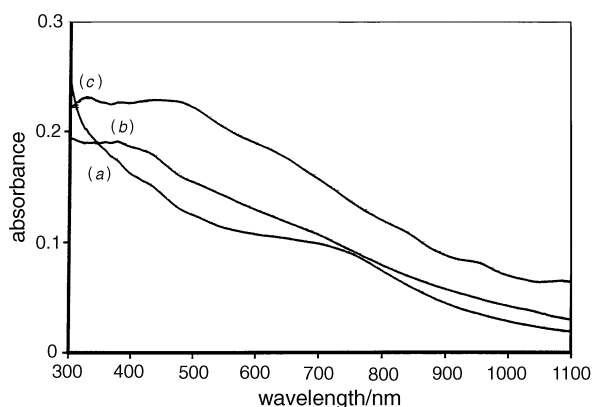


Fig. 3 Optical absorption spectra of nanodispersed PbS in toluene, synthesised in TOPO at 150°C from $\text{Pb}(\text{S}_2\text{CNRR}')_2$ over 1 h: (a) $\text{R} = \text{R}' = \text{Bu}^n$; (b) $\text{R} = \text{Me}$, $\text{R}' = n\text{-C}_6\text{H}_{13}$; (c) $\text{R} = \text{R}' = \text{Bu}^i$

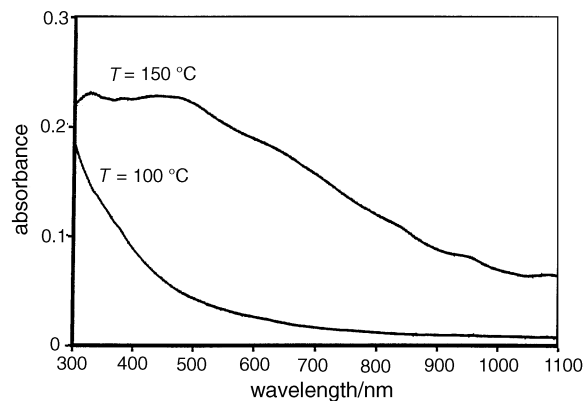


Fig. 4 Optical absorption spectra of nanodispersed PbS in toluene, synthesised from $\text{Pb}(\text{S}_2\text{CNBu}^i)_2$ in TOPO at 100 and 150°C , over 1 h

UV to the NIR (1100 nm) was always observed. Although a sharp edge was not observed in any of the optical spectra, Fig. 3–5 suggest that the PbS particles should have diameters in the nanometre range. The direct optical band-gap of macrocrystalline PbS is *ca.* 0.4 eV (3100 nm); absorption of light from this wavelength to higher energy, forming a continuum, occurs in bulk PbS. This is not the case for nanodispersed PbS described here, as shown in Fig. 3–5.

A blue shift in the absorbance band should occur for PbS nanoparticles of large size ($>20\text{ nm}$) as compared to semiconductors such as II–VI materials. For example, CdS shows a three-dimensional quantum confinement for particles smaller than 60 \AA . However because the bulk exciton radius of PbS is larger than for CdS the former shows quantum size effects for nanoparticles up to 160 \AA in diameter. Although quantum confined semiconductors, such as CdS and CdSe, usually show excitonic features in their optical spectra, for PbS this effect has not been observed so often. Well defined absorption features were reported for molecular-like PbS clusters ($<13\text{ \AA}$) prepared in a polymeric matrix¹¹ and for PbS synthesised in the presence of poly(vinyl alcohol) in methanolic or aqueous solutions.⁹

Morphological and structural properties of PbS nanocrystallites

The PbS nanocrystallites have the cubic (rock-salt type) structure. The transmission electron diffraction pattern of a typical sample showed rings which were indexed to the *d*-spacings of cubic PbS [Fig. 6(b)]. Fig. 6(a) shows the diffraction pattern of a single nanocrystal in which the $\{200\}$ and $\{220\}$ planes were easily assigned.

The HRTEM images of PbS showed crystalline particles

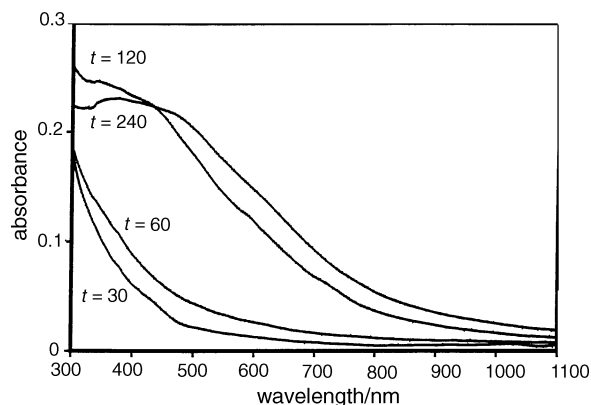


Fig. 5 Optical absorption spectra of nanodispersed PbS, in toluene, synthesised from the thermolysis (100°C) of $\text{Pb}(\text{S}_2\text{CNBu}^i)_2$ in TOPO for different heating times (in minutes)

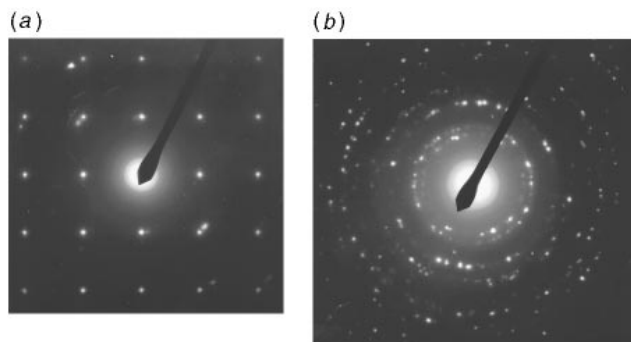


Fig. 6 Transmission electron diffraction patterns of PbS nanocrystallites: (a) single nanocrystal; (b) set of particles

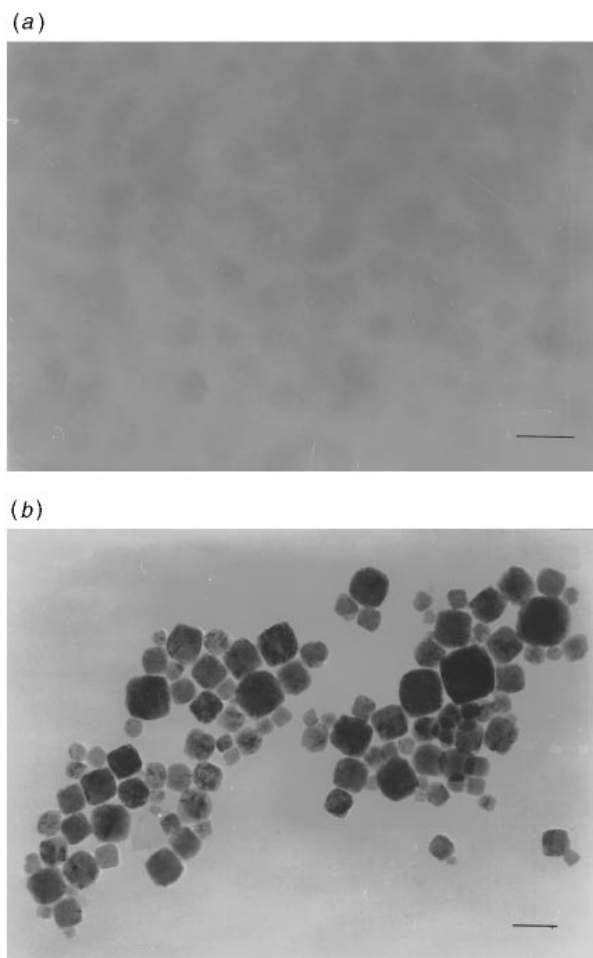


Fig. 7 HRTEM images of PbS nanocrystallites prepared from thermolysis of $\text{Pb}(\text{S}_2\text{CNBu}_2)_2$ in TOPO, over 1 h, at: (a) 100 °C (bar = 10 nm) and (b) 150 °C (bar = 100 nm)

which were mostly nanosized (Fig. 7). It appears that the temperature at which the PbS crystals were prepared had a strong influence on their morphology. Fig. 7 shows PbS nanocrystallites prepared at 100 °C (a) and 150 °C (b), respectively. Closer examination of these crystallites show that not only the morphology, but also the size dispersions differ between the two samples. Most of the crystallites prepared at 100 °C were round in shape and in the quantum size regime ($d = 6.3 \pm 1.4$ nm) for PbS. The size dispersion of the 100 °C sample was ca. 22%. In the sample prepared at 150 °C, on the other hand, in addition to small rounded nanocrystals, a large number of larger and square shaped nanocrystals were also observed, their average size being of the order $d = 85 \pm 23$ nm (measured diagonal of the square). The size dispersion in this

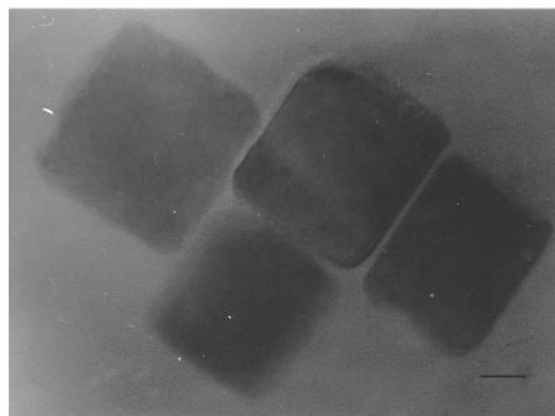


Fig. 8 HRTEM image of PbS nanocrystallites prepared from thermolysis of $\text{Pb}(\text{S}_2\text{CNEt}_2)_2$ in TOPO, over 1 h, at 250 °C (bar = 100 nm)

sample was increased to 27%. The size dispersions of both samples were somewhat broader as compared to CdS or CdSe nanocrystallites prepared under similar conditions.¹⁴

The observed morphology of the PbS crystallites was in accord with the optical measurements which indicated that the crystallites were smaller in the sample prepared at 100 °C as compared to preparation at 150 °C. The large size dispersion in the PbS samples could be the reason for the lack of well defined features in the corresponding optical spectra.

Fig. 8 shows a HRTEM image of PbS crystallites grown in TOPO after thermolysis (250 °C) of the precursor $\text{Pb}(\text{S}_2\text{CNEt}_2)_2$. Two types of morphology were present; most of the crystallites were square while the remainder were hexagonal. On average, the crystallites of the latter group were much larger. This observation suggests that growth of PbS crystallites at 250 °C leads to a very broad size distribution. The corresponding optical spectrum of this sample showed strong light scattering close to the longest wavelength reached by the instrument (1100 nm). These samples were unstable towards agglomeration over a few minutes.

In summary, we have presented a novel and simple method for the preparation of nanodispersed PbS. The optical and morphological properties of the PbS nanocrystallites are strongly dependent on the temperature of synthesis and less so on the chemical nature of the precursor. However, it should be emphasised that only lead(II) dithiocarbamate complexes were studied. The synthetic method can be easily modified for other types of molecular precursors to PbS.

T. T. acknowledges JNICT (Praxis XXI program) for a grant and P. O'B. thanks the EPSRC for support of quantum dot research at ICTMS.

References

- 1 A. Henglein, *Chem. Rev.*, 1989, **89**, 1861.
- 2 M. L. Steigerwald and L. E. Brus, *Acc. Chem. Res.*, 1990, **23**, 183.
- 3 H. Weller, *Adv. Mater.*, 1993, **5**, 88.
- 4 A. Hagfeldt and M. Grätzel, *Chem. Rev.*, 1995, **95**, 49.
- 5 J. H. Fendler and F. C. Meldrum, *Adv. Mater.*, 1995, **7**, 607.
- 6 A. P. Alivisatos, *J. Phys. Chem.*, 1996, **100**, 13226.
- 7 A. J. Nozik, F. Williams, M. T. Nenadovic, T. Rajh and O. I. Micic, *J. Phys. Chem.*, 1985, **89**, 397.
- 8 T. K. Leolidou, W. Caseri and U. W. Suter, *J. Phys. Chem.*, 1994, **98**, 8992.
- 9 S. Gallardo, M. Gutierrez, A. Henglein and E. Janata, *Ber. Bunsen-Ges. Phys. Chem.*, 1989, **93**, 1080.
- 10 Y. Wang and N. Herron, *J. Phys. Chem.*, 1991, **95**, 525.
- 11 Y. Wang, A. Suna, W. Mahler and R. Kasowski, *J. Chem. Phys.*, 1987, **87**, 7315.
- 12 R. Tassoni and R. R. Schrock, *Chem. Mater.*, 1994, **6**, 744.
- 13 M. Moffitt and A. Eisenberg, *Chem. Mater.*, 1995, **7**, 1178.
- 14 T. Trindade and P. O'Brien, *Adv. Mater.*, 1996, **8**, 161.

- 15 C. B. Murray, D. J. Norris and M. G. Bawendi, *J. Am. Chem. Soc.*, 1993, **115**, 8706.
- 16 G. Kräuter, P. Favreau and W. S. Rees, Jr., *Chem. Mater.*, 1994, **6**, 543.
- 17 T. Trindade and P. O'Brien, *Adv. Mater.*, in press.
- 18 R. A. Zingaro and J. C. White, *J. Inorg. Nucl. Chem.*, 1960, **12**, 315.
- 19 G. M. Sheldrick, SHELX, a program for crystal structure solution, University of Göttingen, 1986.
- 20 G. M. Sheldrick, SHELXL-93, program for crystal structure solution, University of Göttingen, 1993.
- 21 M. A. Bernard and M. M. Borel, *Bull. Soc. Chim. Fr.*, 1969, **9**, 3064.
- 22 M. A. Bernard and M. M. Borel, *Bull. Soc. Chim. Fr.*, 1969, **9**, 1966.
- 23 F. Bonati and G. Minghetti, *Chim. Ind. (Milan)*, 1970, **52**, 1204.
- 24 L. A. Kosareva and S. V. Larionov, *Izv. Sib. Otd. Akad. Nauk SSSR, Ser. Khim. Nauk*, 1989, **4**, 33.
- 25 H. Iwasaki, *Acta Crystallogr., Sect. B*, 1980, **36**, 2138.
- 26 Z. V. Zvonkova, A. N. Khvatkina and N. S. Ivanova, *Kristallografiya*, 1967, **12**, 1065.
- 27 H. Iwasaki and H. Hagihara, *Acta Crystallogr., Sect. B*, 1972, **28**, 507.
- 28 M. Ito and H. Iwasaki, *Acta Crystallogr., Sect. B*, 1980, **36**, 443.
- 29 A. J. Bondi, *J. Phys. Chem.*, 1964, **68**, 441.
- 30 S. L. Lawton and G. T. Kokotailo, *Inorg. Chem.*, 1972, **11**, 363.
- 31 H. U. Hummel, E. Fischer, T. Fischer, D. Größ, A. Franke and W. Dietzsch, *Chem. Ber.*, 1992, **125**, 1565.
- 32 F. Bonati and R. Ugo, *J. Organomet. Chem.*, 1967, **10**, 257.
- 33 D. M. Adams and J. B. Cornell, *J. Chem. Soc. A*, 1968, 1299.
- 34 D. M. Adams and J. B. Cornell, *J. Chem. Soc. A*, 1967, 884.
- 35 T. Y. Koh, PhD Thesis, University of London, 1994.
- 36 M. Motevalli, P. O'Brien, J. R. Walsh and I. M. Watson, *Polyhedron*, 1996, **15**, 2801.
- 37 P. O'Brien, J. R. Walsh, I. M. Watson, M. Motevalli and L. Henriksen, *J. Chem. Soc., Dalton Trans.*, 1996, 2491.

Paper 6/08579B; Received 23rd December, 1996